

Published in final edited form as:

*Biochemistry*. 2012 August 14; 51(32): 6388–6399. doi:10.1021/bi300340r.

## ***In Vitro* formation and characterization of the skeletal muscle $\alpha$ - $\beta$ Tropomyosin heterodimers**

Athanasia Kalyva<sup>1,2</sup>, Anja Schmidtman<sup>2</sup>, and Michael A. Geeves<sup>\*</sup>

School of Biosciences, University of Kent, Canterbury, CT2 7NJ, UK

### **Abstract**

Tropomyosin (Tm) is a dimer made of two alpha helical chains associated into a parallel coiled-coil. In mammalian skeletal and cardiac muscle the Tm is expressed from two separate genes to give the  $\alpha$ - and  $\beta$ -Tm isoforms. These associate *in vivo* to form homo ( $\alpha_2$ ) and heterodimers ( $\alpha$ - $\beta$ ) with little  $\beta_2$  normally observed. The proportion of  $\alpha_2$  vs  $\alpha$ - $\beta$  varies across species and across muscle types from almost 100 %  $\alpha_2$ - to 50 %  $\alpha$ - $\beta$ -Tm. The ratio can also vary during development and in disease. The functional significance of the presence of these two isoforms has not been defined because it is difficult to isolate or purify the  $\alpha$ - $\beta$  dimer for functional studies. Here we report an effective method for purifying bacterially expressed Tm as  $\alpha$ - $\beta$  dimers using a cleavable N-terminal tag on one of the two chains. The same method can be used to isolate Tm dimers in which one chain carries a mutation. We go on to show that the  $\alpha$ - $\beta$  dimers differ in key properties (actin affinity, thermal stability) from either the  $\alpha_2$ - or  $\beta_2$ -Tm. However, the ability to regulate myosin binding when combined with cardiac troponin appears unaffected.

### **Keywords**

Protein folding; calcium regulation; muscle contraction; protein isoforms

Tropomyosin (Tm) is a dimeric  $\alpha$ -helical coiled-coil protein that is found associated with actin filaments in the cell (1), where it has a role in stabilizing actin filaments. In skeletal and cardiac muscle cells Tm is associated with the actin filaments of the sarcomere (2) (3) and in association with troponin (Tn) it is a regulator of striated muscle contraction (4). However, the functional role of different Tm isoforms in striated muscle contraction has not been defined.

Mammalian striated muscle expresses two isoforms of tropomyosin, the  $\alpha$ - and the  $\beta$ -isoform, and although products of different genes (*TMPI* and *TPM2* for human and rabbit and *Tpm1* and *Tpm2* for mouse and rat) they are highly comparable in amino acid sequence (for example ~ 86 % identical for rat isoforms). Heart & fast skeletal muscle expresses the same two  $\alpha$ -Tm and  $\beta$ -Tm isoforms (5). All striated muscle cells express  $\alpha$ -Tm and a variable amount of the  $\beta$ -Tm. The two protein isoforms dimerise to form the functional  $\alpha_2$ - and  $\alpha$ - $\beta$ -dimers. The  $\beta_2$  homodimer is rarely found (6) (7). The ratio of  $\alpha_2$ -Tm versus  $\alpha$ - $\beta$ -Tm in muscles is highly variable and depends upon the muscle type (2) (8) and the size of

<sup>\*</sup>Address correspondence to School of Biosciences, University of Kent, UK; Tel +44 1227 827597; Fax: +44 1227 763912; M.A.Geeves@kent.ac.uk. .

<sup>1</sup>Current address Institute of Human Performance and Rehabilitation, Karies, Trikala, Greece.

<sup>2</sup>These authors contributed equally to this work.

**Supporting Information Available** The supplemental figures show thermal unfolding curves and their 1<sup>st</sup> derivatives of tagged Tm dimers and SDS gels of cross-linked dimers run in the presence of DTT. This material is available free of charge via the Internet at <http://pubs.acs.org>.

the organism (reviewed in (3)) i.e.  $\alpha_2$ -Tm is more common in smaller mammals (9) and faster muscles (8). In the heart muscle the  $\alpha_2$ -Tm homodimer is the predominant isoform in small animals like rabbit, guinea pig and rat which have a faster heartbeat. In contrast, pig, sheep and human hearts that beat more slowly have up to 20 % of the  $\beta$ -Tm isoform present as  $\alpha$ - $\beta$ -Tm (9) (10). Of note is the observation that artificially induced pressure overload by aortic coarctation in rats causes the re-expression of the  $\beta$ -Tm gene in the ventricular myocardium (11). Following up this observation Muthuchamy et al. over-expressed  $\beta$ -Tm in transgenic mice (12). Although  $\beta$ -Tm protein made up to ~ 58 % of the Tm content in the myocytes and formed almost entirely  $\alpha$ - $\beta$  heterodimers its overexpression had no effect on the cardiomyocyte structure nor on their overall performance except for an increase in the rate of relaxation (12). However, when  $\beta$ -Tm was more than 75 % of the overall Tm content of mouse cardiomyocytes these cardiomyocytes showed histological abnormalities and impaired contraction and relaxation and the transgenic mice died 10-14 days after birth (13). These cardiac muscle studies suggest that the different tropomyosin isoforms have distinct functional properties. What these properties are and how they affect muscle physiology remains to be defined.

Although  $\beta_2$ -Tm is unstable at the physiological temperature of 37 °C (14) (15), at the normal temperatures of *in vitro* measurements (<20 °C)  $\beta_2$ -Tm is stable. This allowed functional differences between  $\alpha_2$ - and the non-physiological  $\beta_2$ -Tm to be examined and showed a small change in the affinity of the different Tm for actin (0.18  $\mu$ M for  $\alpha_2$ -Tm; 0.23  $\mu$ M for  $\beta_2$ -Tm; (16)). Compared to  $\alpha_2$ -Tm,  $\beta_2$ -Tm also showed a small increase (0.2 pCa units) in the calcium sensitivity when reconstituted with cardiac Tn but not skeletal muscle Tn (16). These differences could potentially be quite distinct in the  $\alpha$ - $\beta$ -Tm. However, studies of the functional role of  $\alpha$ - $\beta$ -Tm have been hindered by the difficulty of isolating or reconstituting the  $\alpha$ - $\beta$ -Tm. No skeletal muscle has been shown to express exclusively the heterodimer so that any tissue purified material results in a heterogeneous mixture of  $\alpha_2$ - and  $\alpha$ - $\beta$ -Tm. Separation of the  $\alpha_2$ - and  $\alpha$ - $\beta$ -Tm dimers is possible on an hydroxyapatite column (17) but we have found it unreliable for large quantities of protein. We found that bacterial expression of  $\alpha$ - and  $\beta$ -Tm either co-expressed or recombined results again in a heterogeneous mixture of the two homodimers and heterodimers after purification. This observation for striated muscle Tm is in contrast to experiments with smooth muscle Tm which preferentially assemble at physiological temperatures into the  $\alpha$ - $\beta$ -Tm (18) (19).

Here we present for the first time a reproducible method for the *in vitro* formation of the skeletal muscle  $\alpha$ - $\beta$ -Tm heterodimer. We use separate bacterially expressed  $\alpha_2$ - and  $\beta_2$ -Tm in which the recombinant  $\beta_2$ -Tm carries an N-terminal affinity tag that can be removed after the purification of the heterodimer from the homodimers. Proteolytic cleavage of the tag resulted in a functional Tm heterodimer. We go on to show that there is little differences between  $\alpha_2$ - &  $\alpha$ - $\beta$ -Tm dimers in their affinity for actin or in the  $\text{Ca}^{2+}$  regulation of myosin binding to actin. However, the heterodimer appeared distinct in its thermal stability to either  $\alpha_2$ - or  $\beta_2$ -Tm.

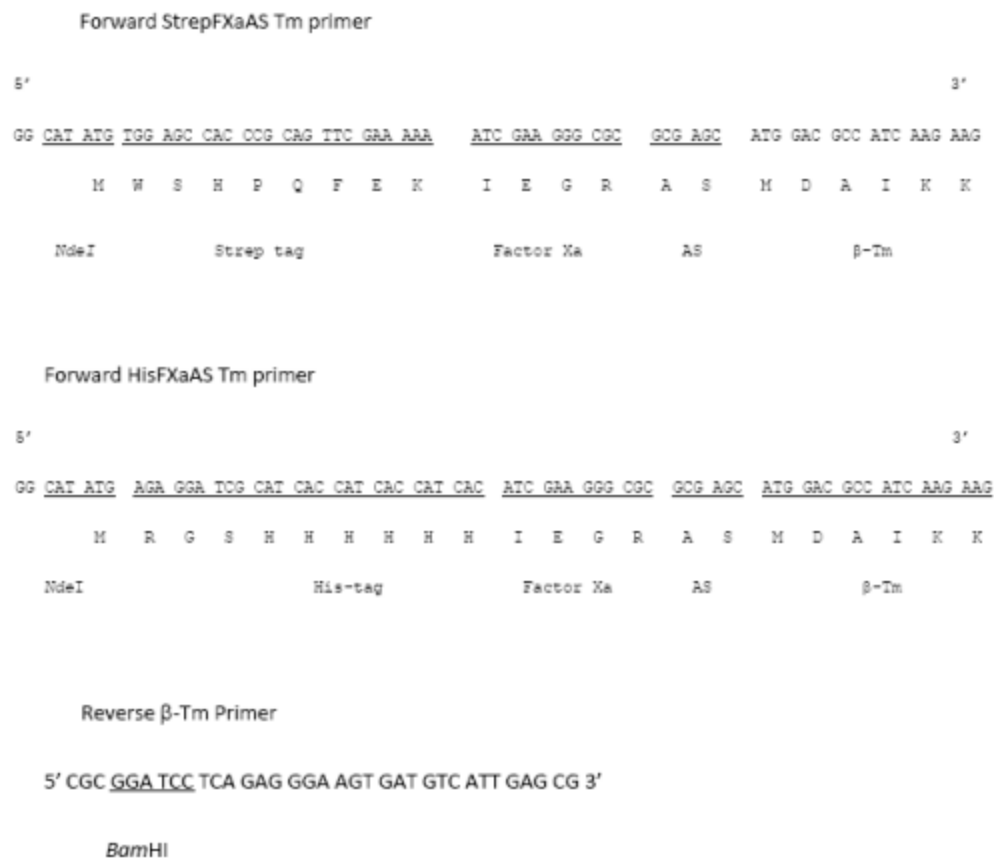
## Experimental Procedures

### Plasmid construction

Rat skeletal  $\beta$ -Tm (gene: Tpm2) was generated with the addition of either a Strep-tag; Sequence: Trp-Ser-His-Pro-Gln-Phe-Glu-Lys (20)) or a His<sub>6</sub>-affinity tag (Sequence: Arg-Gly-Ser-His-His-His-His-His). Both tag sequences were followed by the Ile-Glu-Gly-Arg sequence, which is the recognition site for the Factor Xa protease (21). Both, the  $\alpha$ - &  $\beta$ - rat Tm, had the Ala-Ser N-terminal extension required to mimic the N-terminal

acetylation for a functional Tm (22). The rat  $\alpha$ -Tm was used with the Ala-Ser extension as described by Kremneva et al. (23).

For the addition of the DNA-sequence coding for the His- or Strep-Tag, plus the Factor Xa-restriction site to the 5' end of  $\beta$ -Tm sequence we used the polymerase chain reaction (PCR) according to Sambrook *et al.* (24), with the following set of primers:



As template DNA we used the rat skeletal  $\beta$ -Tm with an N-terminal Ala-Ser extension, subcloned into a pJC20 vector (16). Note that the rat Tm sequences are identical to the human sequences except for a single conservative change in each chain. Lys-220 is Arg in human  $\alpha$ -Tm while Asp-66 is Glu in human  $\beta$ -Tm. The PCR product was subcloned into the pGEM-T Easy cloning vector (Promega Corporation, UK) following the manufacturers' instructions. The insert was cut out from the pGEM-T Easy cloning vector via the *Nde*I and *Bam*HI restriction sites and finally subcloned into the pJC20 expression vector (25).

### Protein expression

The expression and harvesting of all recombinant proteins is described in detail by Coulton et al. (26). The recombinant  $\alpha$ -Tm and  $\beta$ -Tm (without tag but with the N-terminal Ala-Ser extension (16)) were purified by ion exchange chromatography as described by Coulton et al. (27) with minor differences. Instead of the Pharmacia HiTrap-Q column we used HiTrap Q HP columns (GE Healthcare) and we eluted with a steady gradient from 100 mM to 1 M KCl. Purification yield was approximately 40 mg/L of bacterial culture.

The cells expressing either Strep-tagged  $\beta$ -Tm (Strep $\beta$ -Tm) or His-tagged  $\beta$ -Tm (His $\beta$ -Tm) were both harvested and resuspended in lysis buffer and lysed by sonication, as described

for  $\alpha$ - and  $\beta$ -Tm. After the sonication the cells were centrifuged at  $355000 \times g$  for 20 minutes and the soluble Tm in the supernatant was isoelectrically precipitated at pH 4.7 for Strep $\beta$ -Tm or pH 4.8 for His $\beta$ -Tm. The precipitate was centrifuged at  $3700 \times g$  for 10 minutes and the pellet containing Strep $\beta$ -Tm was resuspended in wash buffer (100 mM Tris, pH 8.0, 150 mM NaCl, 1 mM EDTA) and 10 mg/L DNase and 10 mg/L RNase were added. After a 2 h incubation at 4 °C the sample was transferred to a Strep-Tactin Sepharose column (IBA GmbH, Germany). Unbound protein was washed off by applying 5 column volumes (CV) of wash buffer. The bound Strep-tagged Tm was eluted by applying 3 CV of wash buffer with 2.5 mM desthiobiotin. The yield of the Strep-tagged Tm using a 5 ml Strep-Tactin gravity column was  $\sim 20$  mg/L of bacterial culture and the purified Strep $\beta$ -Tm was stored in High Salt Buffer (20 mM KPi, pH 7.0, 0.5 M KCl, 5 mM MgCl<sub>2</sub>) at  $-20$  °C. The Strep $\beta$ -Tm protein concentration for the dimer was determined from its absorption at 280 nm using a molecular extinction coefficient of  $\epsilon_{280} = 29130 \text{ l mol}^{-1} \text{ cm}^{-1}$ .

Pellets containing precipitated His $\beta$ -Tm were resuspended with High Salt Buffer and 10 mg/L DNase and 10 mg/L RNase were added. The sample was incubated at 4 °C for 2 h and then loaded onto a Ni-NTA column (QIAGEN Ltd., Germany). The column was washed with 4 CV of 0.3 M NaCl, 50 mM NaH<sub>2</sub>PO<sub>4</sub>, pH 8.0, 20 mM imidazole and His $\beta$ -Tm was eluted by washing with 6 CV of buffer with imidazole increased to 250 mM. The purification yield of His $\beta$ -Tm using a 10 ml Ni-NTA gravity column was  $\sim 20$  mg/L bacterial culture and the purified His-tagged protein was stored in the High Salt Buffer at  $-20$  °C. The His $\beta$ -Tm dimer concentration was determined from its absorption at 280 nm using its molecular extinction coefficient of  $\epsilon_{280} = 18130 \text{ l mol}^{-1} \text{ cm}^{-1}$ .

The mass of the purified proteins was determined either on the LC-Q (Thermo Finnigan) or the micrOTOF-Q II (Bruker) and was 32838.48 Da for  $\alpha$ -Tm (estimated 32838.7), 32995.3 Da for  $\beta$ -Tm (estimated 32994.8), 34704.72 Da for His $\beta$ -Tm (estimated 34704.7) and 34621.65 Da for Strep $\beta$ -Tm (estimated 34621.7).

### Formation of skeletal $\alpha$ - $\beta$ -Tm

To form Tm heterodimers we followed the protocol described by Coulton et al. (26) with minor differences. The procedure is summarized schematically in Figure 1 and is described in detail in the Results section.

### Separation of proteins by SDS-PAGE

Protein samples were analyzed by SDS polyacrylamide gel electrophoresis. Depending on the resolution required we used either a 7.5 % (w/v) or 10 % (w/v) acrylamide gel. For samples run under non-reducing conditions we added 5x sample buffer (0.625 M Tris, pH 6.8, 40 % Glycerol, 10 % SDS, 0.005 % Bromphenol blue) and loaded the samples straight onto the gel. For samples run under reducing conditions we used the same recipe for the sample buffer but added 10 % (v/v) 2-mercaptoethanol and incubated the samples for at least 5 minutes at  $\sim 90$  °C before loading. As protein ladders we either used a kaleidoscope prestained standard (ranging from 200 to 6.5 kDa from BioRad) or the PageRuler<sup>TM</sup> prestained protein ladder (Fermentas). Recipes for resolving gel, stacking gel, electrode buffer and sample buffer are adopted from the standard Laemmli recipe (28). We also used NuPAGE<sup>®</sup> 4-12 % Bis-Tris Gel in combination with NuPAGE MOPS running buffer (both Invitrogen).

### Purification of skeletal $\alpha$ - $\beta$ -Tm heterodimer

After assembly of the heterodimers the sample contained a mixture of cross-linked untagged  $\alpha_2$ -Tm, the single-tagged  $\alpha$ - $\beta$ -Tm and double-tagged  $\beta_2$ -Tm. These were separated using the Tags in affinity chromatography. Samples containing Strep-tagged  $\beta$ -Tm were loaded onto a

10 mL Strep-Tactin Sepharose column. Unbound protein was washed off by applying 10 CV of wash buffer. Strep-tagged heterodimers were eluted with a linear gradient of 0 - 2.5 mM desthiobiotin in wash buffer.

The His-tagged heterodimers were loaded onto a 10 mL Ni-NTA column (QIAGEN Ltd., Germany). The untagged  $\alpha_2$ -Tm did not bind to the column. The column was washed with 20 mM imidazole in 300 mM NaCl, 50 mM NaH<sub>2</sub>PO<sub>4</sub>, pH 8.0 to remove unbound protein. The His-tagged heterodimers were eluted at 50 mM imidazole in 300 mM NaCl, 50 mM NaH<sub>2</sub>PO<sub>4</sub>, pH 8.0. For the elution of double-tagged homodimers high concentration of imidazole (250 mM) were used. Samples were visualized using non-reducing SDS gels. Samples which contained a mixture of non-tagged homodimers with single tagged heterodimers were collected and subjected to further purification cycles. Samples containing mostly the heterodimer were pooled together.

Finally the affinity tags were removed by incubating with FXa protease (30 units/mg of protein; QIAGEN Ltd., Germany) at room temperature overnight.

### Thermal unfolding of Tm using Circular Dichroism

The Circular Dichroism at 222 nm was recorded for each of the Tm samples over a temperature range from 5 °C to 65 °C (1 °C/minute) using a peltier device (Jasco PTC 423S/15) in a stoppered 1 mm cuvette (Starna Scientific Ltd.) with a Jasco 715 Spectropolarimeter, UK (software: spectra management V1.51.00). The Tm samples were diluted to a final concentration of 5-10  $\mu$ M in 20 mM KPi, pH 7.0, 0.5 M NaCl and 5 mM MgCl<sub>2</sub>. The temperature scans for each sample were repeated 3 times, then 1 mM DTT was added and the scans were repeated a further three times. For all samples scan number 2 & 3 were identical and scan number 5 & 6 were identical. To define the unfolding “domains” the melting curves were smoothed (Savitzky-Golay method; 50 points of window, 301 points in total) and the first derivative was calculated, then multiple Gaussian peaks were fitted using MicroCal Origin 8 software.

### Proteins

Actin and myosin S1 were purified from rabbit skeletal tissue following protocols from Spudich & Watt (29) and Margossian & Lowey (30), respectively. Cardiac troponin was a kind gift of Dr. K. Jaquet (Ruhr Universitaet Bochum, Germany). For the kinetic experiments actin was labelled at Cys374 with pyrene iodoacetamide (31) and stabilized by incubating in a 1 : 1 ratio with phalloidin.

### Cosedimentation

The affinity of each Tm dimer for actin was estimated using a cosedimentation assay. The general protocol is described by Coulton et al. (26). Actin at 7 - 10  $\mu$ M was incubated with increasing concentrations of Tm (0 to 5  $\mu$ M) at 20 °C in 20 mM MOPS, pH 7.0, 100 mM KCl, 5 mM MgCl<sub>2</sub>. After 1 h incubation the actin was pelleted with any bound Tm by ultracentrifugation at 370000  $\times g$  for 20 minutes. Equivalent samples of the pellet and the supernatant were run on a SDS-PAGE. SDS-gels were scanned (Epson Perfection V750 Pro) and the scanned images were analyzed with ScionImage software (Scion Corp., Frederick, MD). The free Tm concentration was plotted against the fractional actin saturation,  $\theta$ , and the sigmoidal curve, which indicates Tm polymerizing on to actin (32), was fitted to the Hill equation  $\theta = [\text{Tm}]^n / (K50\%^n + [\text{Tm}]^n)$  with  $n$ , the Hill coefficient and K50%, the midpoint of the curve, using MicroCal Origin 8 software.

## The kinetics of S1 binding to actinTmTn

The rate of S1 binding to actin-Tm-Tn-filaments under pseudo first order conditions ( $[S1] \gg [actin]$ ) was recorded by monitoring the change in pyrene actin fluorescence (16). Pyrene was excited at 365 nm and the fluorescence emitted detected through a 389 nm cut off filter using a SF-61DX2 spectrophotometer (HiTech Scientific). The data was analyzed using the Kinetassist software. For the reconstitution of the thin filament 4  $\mu$ M phalloidin stabilized actin was incubated for 30 minutes with Tm and human cardiac Tn in a ratio of 7 : 2 : 3 or 7 : 4 : 4 to ensure the full saturation of the actin filament. The reaction was recorded in the absence (+ 2 mM EGTA) or presence (+ 2 mM CaEGTA) of  $Ca^{2+}$ , in 100 mM KCl, 5 mM  $MgCl_2$ , 20 mM MOPS, pH 7.0 at 20 °C.

## Results

### In vitro formation and isolation of the skeletal $\alpha$ - $\beta$ -Tm

The protocol for formation and isolation of the  $\alpha$ - $\beta$ -Tm heterodimer is outlined in Fig. 1. Initially two separate batches of bacterially expressed  $\alpha_2$  and tagged- $\beta_2$  homodimers were treated with DTT at 58 °C for 10 min to eliminate disulphide cross-bridges and to separate the Tm dimer into monomers. The two sets of monomers were then combined at 58 °C, then cooled down to 37 °C and incubated at this temperature for 45 minutes to allow dimer formation before storing on ice. Heterodimer formation was assessed by cross-linking the two chains via the Cys residues and analyzing by gel electrophoresis under non reducing conditions. To do this DTT was removed via gel filtration and then the sample was incubated with 10 mM  $K_3Fe(CN)_6$  and 2  $\mu$ M  $CuSO_4$  at 37 °C to catalyse the oxidation of the Cys side chains (19).  $\alpha$ -Tm has a Cys at position 190 and  $\beta$ -Tm has two Cys at positions 36 and 190. Thus  $\alpha_2$ -Tm and  $\alpha$ - $\beta$ -Tm can form disulfide bonds at Cys190 and the  $\beta_2$ -Tm can form single or double disulfide bonds at Cys36 and Cys190. Other cross-links are possible but are relatively rare in Tm. We need to ensure 100 % dimer cross-linking to assess how much heterodimer is formed. The incubation time required to complete the cross-linking was surprisingly variable from sample to sample and we used incubation times from 2 to 18 h. Figure 2 shows a 7.5 % (w/v) SDS non-reducing gel of the control  $\alpha_2$ - (lane 2) and tagged- $\beta_2$ -Tm (lane 4) and the mixed  $\alpha$  and  $\beta$  Tm sample (lane 3). All three samples have been through the heating and re-annealing and oxidation steps. The  $\alpha_2$ - and tagged- $\beta_2$ -Tm run as distinct bands on the gel and the mixture of  $\alpha$ - and tagged- $\beta$ -Tm shows the presence of a new band that runs between the  $\alpha_2$ - and tagged- $\beta_2$ -Tm bands indicating the  $\alpha$ - $\beta$ -Tm dimer with a single tag. The gel is run for a long time to give a clear separation of the dimers at heavy loading to illustrate the higher molecular weight adducts. No monomers are present if the gel is run for a shorter time. If the samples before and after oxidation treatment are run on a SDS-gel under reducing conditions only the  $\alpha$ - and  $\beta$ -monomer bands are seen (see supplemental Fig.S2) indicating a small amount of high molecular weight species but no major oxidation adducts in the sample. When mixing  $\alpha_2$ - and tagged- $\beta_2$ -Tm in a ratio of 1 : 1 we observed dimers in the proportion of approximately 40 %  $\alpha_2$ , 20 %  $\alpha$ - $\beta$  and 40 %  $\beta_2$ . A random assembly of dimers would predict ratios of 1 : 2 : 1 suggesting a ~ 2-fold preference for the assembly of homodimers over the heterodimer. We routinely use a 3 : 1 starting mixture of  $\alpha_2$ - and His- $\beta_2$ -Tm and 6 : 1 starting mixture of  $\alpha_2$ - and Strep- $\beta_2$ -Tm, as this increased the yield of  $\alpha$ - $\beta$ -Tm heterodimer after purification (see below).

The oxidation step is quite a harsh treatment but is essential if defined 100% heterodimers are to be formed for later use. It is possible that uncross-linked dimers could exchange partners over time. However the protein can be purified without cross-linking and the presence of the heterodimer can be checked at any stage by taking a sample, oxidizing it and running on a non-reducing gel. We routinely used the cross-linked sample in most of the

experiments and control measurements showed if there was any difference in the behavior of native vs cross-linked samples.

In the next step the  $\alpha$ -tagged- $\beta$ -Tm was separated from the  $\alpha_2$ - and tagged- $\beta_2$ -Tm by affinity chromatography. The mixture was applied to either a NiNTA column for His-tagged dimers or a Strep-Tactin Sepharose column for Strep-tagged dimers. Figure 3 shows the elution profile for the Strep-tagged preparation. The untagged  $\alpha_2$ -Tm was not retained by the column and was collected in the wash for future use, since these fractions still contained some single tagged  $\alpha$ - $\beta$ -Tm (Fig. 3, fraction 3 - 29). The isolated  $\alpha$ -tagged- $\beta$ -Tm was eluted at  $\sim 1.75$  mM desthiobiotin (Fig. 3) followed by a mixture of  $\alpha$ -tagged- $\beta$ - and tagged- $\beta_2$ -Tm with increasing concentration of desthiobiotin in the elution buffer (Fig. 3). Note that fraction 52 shows no sign of the tagged- $\beta_2$ -Tm but it does appear from fraction 56 onwards. The presence of  $\beta_2$  cannot be assessed in lanes 53-55 because of the large amount of  $\alpha$ - $\beta$ -Tm present. The purity of the final product is assessed in Fig 4 (below). We used as standard a 6 : 1 mixture of  $\alpha_2$ - to  $\beta_2$ -Tm in the starting sample resulting mostly in  $\alpha_2$ - and  $\alpha$ -tagged- $\beta$ -Tm dimers after thermal treatment making the isolation of the tagged heterodimer from the double tagged- $\beta_2$  homodimer more efficient but note that a small contaminant of a band running at the  $\alpha_2$ -Tm position is carried through.

The purified  $\alpha$ -tagged- $\beta$ -Tm was checked by SDS-PAGE under both reducing and non-reducing conditions (Fig. 4a, lane 3 and 7, respectively). It can be observed that running the heterodimer sample under non-reducing conditions showed a single band of the expected size of the dimer (Fig. 4, lane 7). When reducing conditions were used, two distinct bands of the expected monomeric components were observed which were of similar density corresponding to the expected 1 : 1 ratio of  $\alpha$  and  $\beta$  monomers arising from the heterodimer (Fig. 4, lane 3). Gel densitometry limits any contaminant of  $\beta\beta$  or  $\alpha\alpha$  to  $<5\%$  the limit of the precision of the analysis. The purity of the final sample is further checked by running a heavily loaded gel under non-reducing conditions, Fig 4b. This shows a single large band – no evidence of a  $\beta_2$ -Tm band with a small band of  $\sim 7\%$  running in the position of  $\alpha_2$ -Tm.

In the final step the tag was proteolytically cleaved from the  $\alpha$ -tagged  $\beta$ -Tm by using FXa protease digestions. Running the protease treated  $\alpha$ - $\beta$ -Tm sample under non-reducing conditions showed a single band which runs faster than the  $\alpha$ -tagged- $\beta$ -Tm sample (Fig. 4 lane 8 and 7, respectively). When the sample was run under reducing conditions two distinct bands with similar density were observed. These two bands run on the same position as  $\alpha$ -Tm and untagged  $\beta$ -Tm (Fig. 4, lane 5, 4 and 6, respectively). The yield of heterodimer was 0.75 - 1.5 mg from a starting mixture of 5 mg of Strep-tagged -  $\beta$ -Tm and 30 mg of  $\alpha$ -Tm.

Identity and purity of the cross-linked  $\alpha$ - $\beta$  heterodimers was confirmed by mass spectrometry with a mass peak for the  $\alpha$ - $\beta$  dimer of 65,832 Da, as expected..

### Thermal stability

The thermal stability of each Tm dimer was assessed using circular dichroism. Figure 5A shows the typical CD spectra of  $10 \mu\text{M}$   $\alpha_2$ -Tm with the classical double negative peaks at 208 & 222 nm characteristic of an alpha helical coiled-coil protein. The CD spectra recorded at  $5^\circ\text{C}$  were identical for all Tm samples analyzed. These peaks were largely lost at  $65^\circ\text{C}$  indicating loss of the helical structure. Fig. 5B shows the unfolding profile of  $\alpha_2$ -Tm over the range of 5 to  $65^\circ\text{C}$  at 222 nm. The unfolding of Tm was reversible and the unfolding profile was repeated six times for each sample with little loss of the total signal. The first three scans were collected in the absence of DTT and show the unfolding of the thiol cross-linked dimer. Scans 2 & 3 were always identical with occasional variation in scan 1. This may represent the presence of a variable amount of non-cross linked dimer in the starting material. 1 mM DTT was added before scan 4 and the scan shows the thermal effect of both,

Tm unfolding and the gradual loss of the cross-link. Scans 5 & 6 show the isotherm of the non-cross-linked material (reduced during scan 4) and were, in all cases identical. As shown in Fig. 5B for  $\alpha_2$ -Tm the loss of a single cross-link at Cys 190 results in a significant ( $\sim 10$  °C) loss of stability for the major unfolding transition shifting from  $\sim 57$  to  $47$  °C with a small increase in stability around  $35$  °C. The curves are analyzed in more detail in Figure 6.

Figure 5C compares the thermal unfolding for  $\alpha_2$ -,  $\beta_2$ - and  $\alpha$ - $\beta$ -Tm in the absence of DTT i.e. of the cross-linked dimers. The predicted melting profile if the  $\alpha$ - $\beta$ -Tm was a simple addition of 50 % of each homodimer is added for illustration. Note that as expected the  $\beta_2$ -Tm is less stable than the  $\alpha_2$ -Tm and at  $\sim 42$  °C  $\beta_2$ -Tm has lost 50 % of the CD signal. In contrast  $\alpha_2$ -Tm does not reach the 50 % unfolding point until  $\sim 52$  °C. The  $\alpha$ - $\beta$ -Tm is intermediate between the homodimers and is 50 % unfolded at  $\sim 49$  °C, which is higher than the prediction for a simple arithmetic mean of the two homodimers. Note that this enhanced stability of the heterodimer above the simple predicted value may be greater as the  $\beta_2$ -Tm is stabilized by 2 cross-links compared to a single cross-link for  $\alpha_2$ - and  $\alpha$ - $\beta$ -Tm (see Fig. 1).

Fig. 5D shows the unfolding profile observed for the same samples in the presence of DTT after reduction of the cross-link, i.e. scans 6. In all cases the Tm is less stable after DTT treatment, as expected, but a similar pattern to that in the absence of DTT is observed.  $\alpha_2$ -Tm is the most stable with a mid point at about  $47$  °C while  $\beta_2$ -Tm is 50 % unfolded at  $\sim 40$  °C. The  $\alpha$ - $\beta$ -Tm appears to have a similar 50 % unfolding point to the  $\beta_2$ -Tm but is less stable below the midpoint and more stable above the midpoint than  $\beta_2$ -Tm. The data are analyzed in more detail below, however note that the  $\alpha$ - $\beta$ -Tm after melting with DTT will re-anneal into a mixture of  $\alpha_2$ -,  $\alpha$ - $\beta$ - and  $\beta_2$ -Tm in proportions shown to be approximately 2 : 1 : 2, respectively. As a control we used a purified  $\alpha$ - $\beta$ -Tm sample that had not been through the oxidation step and the melting isotherm was indistinguishable from that of the sample shown in Fig 5D.

The unfolding 'domains' of Tm can be observed more clearly when the curves are plotted as the 1<sup>st</sup> derivative. Figure 6 shows the smoothed differentiated curve (thick grey) with the best fit to Gaussian peaks superimposed and the individual Gaussians shown as dotted lines. Details of each fit are given in Table 1. The error imposed in this process is such that the details of the numbers cannot be relied upon but here we focus on the general effect of the different constructs rather than the details of each domain. {Footnote: It is not strictly correct to refer to the Tm unfolding domains as there are no distinct structural domains in Tm. However there do appear to be distinct regions of Tm that unfold together.}

In the absence of DTT  $\alpha_2$ -Tm thermal unfolding can be described by 3 domains with a major transition at  $57.5$  °C, a smaller shoulder that is not well resolved centered at  $52$  °C and a domain at  $32$  °C (Fig. 6A).  $\beta_2$ -Tm in contrast has a similar transition at  $58$  °C but with a much smaller area and a dominant large broad peak centered at  $41$  °C (Fig. 6C). The  $\alpha$ - $\beta$ -Tm has the same two upper transitions as the  $\alpha_2$ -Tm at  $58$  and  $52$  °C. A peak at lower temperature is present and as for  $\beta_2$ -Tm this peak is very broad but smaller and therefore not well defined (Fig. 6E). This lower peak differs the most between the observed transition and that predicted from the sum of the  $\alpha_2$ -Tm and  $\beta_2$ -Tm analysis (Fig. 6G).

Analysis of the unfolding after treatment with DTT are also shown in Fig. 6 and Table 1. The  $\alpha_2$ -Tm shows domains including a large narrow peak at  $48$  °C with a shoulder at  $54$  °C and a very broad transition centered at  $38$  °C (Fig. 6B). Previous studies have suggested that the domain at  $52$  -  $54$  °C is the N-terminal part of Tm and is independent of the crosslink (23) (33). The C-terminal region unfolds at  $48$  °C and is stabilized by  $10$  °C to  $57.5$  °C by the crosslink. The data here is compatible with that assignment. For  $\beta_2$ -Tm in contrast the 2 peaks observed-with cross linked material can be analyzed as 4 peaks after DTT treatment



(Fig. 6D). As for  $\alpha_2$ -Tm the most stable domain is 10 °C less stable after the DTT treatment and by analogy with the  $\alpha_2$ -Tm could represent to C-terminal region. The broad single domain stabilized by the crosslink at 41 °C splits into 3 bands at 18, 33 and 39 °C after DTT treatment. This suggests the cross link at Cys36 stabilizes a broad region. The presence of the Strep-tag appears to result in merging of the two middle peaks into a single broad transition at 40 °C (Supp material & Table 1).

Analysis of the  $\alpha$ - $\beta$ -Tm after treatment with DTT (Fig. 6F) is difficult as the reduction of the cross-links requires high temperature treatment that also separates the Tm into monomers. After cooling, a heterogeneous mixture of  $\alpha_2$ -,  $\beta_2$ - and  $\alpha$ - $\beta$ -Tm is produced and since there is a 1 : 1 ratio of  $\alpha$  and  $\beta$  monomers we expect a 2 : 1 : 2 mixture of  $\alpha_2$  :  $\alpha$ - $\beta$  :  $\beta_2$  after reannealing.

The most stable domain in the  $\alpha$ - $\beta$ -Tm sample unfolds at 53 °C and corresponds to the most stable domain in the  $\alpha_2$ -Tm. The second domain at 46.6 °C is common to both  $\alpha_2$ - and  $\beta_2$ -Tm. The third domain (38.3 °C), although present as a broad peak in the  $\alpha_2$ -Tm (37.9 °C) and as a small peak in the  $\beta_2$ -Tm (39 °C), has a much bigger area in the  $\alpha$ - $\beta$ -Tm sample and dominates the profile. A fourth very broad peak at 23 °C is also seen. Thus while we cannot state that some domains are entirely due to the  $\alpha_2$ - and  $\beta_2$ -Tm in the mixture the increase in the domain at ~38 °C is certainly a new feature of the  $\alpha$ - $\beta$ -Tm and in Fig. 5D defines the loss of stability compared to  $\alpha_2$ -Tm in this region. In principle we can subtract the unfolding domains expected for 40 %  $\alpha_2$ - and 40 %  $\beta_2$ -Tm from the data to leave just the  $\alpha$ - $\beta$ -Tm. But the subtraction is the major proportion of the total so the errors are very large. The best fit of  $\alpha_2$  +  $\beta_2$ -Tm to the most stable part of the  $\alpha$ - $\beta$ -Tm plot is shown in Fig. 6F (dark line). This corresponds to 32.5 %  $\alpha_2$ - and 32.5 %  $\beta_2$ -Tm and when subtracted from the plot of Fig. F gives small domains at 54 and 42 °C and a larger domain at ~ 36 °C and a broad low temperature domain centered at 25 °C (Fig. 6H).

The supplementary material shows the equivalent unfolding profiles of the proteins before the Strep tag removal and their analysis is summarized in Table 1. The effect of the Strep tag on the unfolding profiles of cross-linked  $\beta_2$ -Tm is to induce a new domain in the middle of the unfolding profile at ~47.5 °C. After DTT treatment the major domain at ~40 °C remains unaffected but elsewhere there is a 10 °C loss of stability as seen for the untagged protein. The two middle domains in the absence of the tag (33 & 39 °C) merge into a single domain at 41 °C (Fig. S1 A, B). The His-tagged proteins behaved almost identically to the Strep-tagged proteins and are not shown.

The presence of the Strep tag in  $\alpha$ - $\beta$ -Tm (-DTT) produces again an increased area on the domain with mid range stability. Here the same 3 domains are observed as in the absence of the tag but the area of the more stable domains is increased by the tag. When treated with DTT the two most stable domains in the absence of the tag (47 & 53 °C) coalesce into a double domain centered at 48 °C with little change in the lower peaks. Subtracting 32.5 % of the ( $\alpha_2$  + double tagged- $\beta_2$ ) signal (dark line in Fig S1F) from the  $\alpha$ -Strep $\beta$ -Tm data leaves a single domain centered at 48 °C (Fig S1H). Overall the presence of the Tag has little effect on the unfolding of the dimer but the additional stability gives a cleaner simpler heterodimer pattern.

### The affinity of $\alpha$ - $\beta$ -Tm heterodimer for filamentous actin

The binding affinities of the  $\alpha$ - $\beta$ -Tm and the  $\alpha_2$ - and  $\beta_2$ -Tm to actin were estimated using the actin cosedimentation assays, according to the literature (16). As shown in Fig. 7, actin at 7  $\mu$ M was incubated with varying concentrations of  $\alpha$ - $\beta$ -Tm and then sedimented by centrifugation. An SDS-gel of samples of the pellet and supernatant (Fig. 7A) allowed the fraction of the Tm associating with actin to be estimated. Note that using the  $\alpha$ - $\beta$ -Tm

heterodimer resulted in two Tm bands of equal density on the SDS-gel, since a reducing SDS-PAGE was performed. Plotting the concentration of free Tm against the Tm bound to actin gives the expected sigmoid curve, consistent with polymerization of Tm onto the actin filament. In Figure 7B the binding curve of  $\alpha$ - $\beta$ -Tm is compared to those of the two homodimers. From the best fit to the Hill equation the apparent affinity of Tm for actin ( $K_{50\%}$ ) and the Hill coefficient ( $n$ ) of binding were estimated. Each curve in Figure 7B originates from an individual experiment, while the mean values of at least three individual experiments for each type of dimer were calculated and are summarized in Table 2. These show that the heterodimer has a weaker  $K_{50\%}$  than the two homodimers ( $p < 0.05$ ) with  $\beta_2$ -Tm having a tighter affinity. The apparent cooperativity is not well defined in these measurements.

### Tm regulation of S1 binding to actin

Figure 8 shows the result of the binding of an excess of S1 to the actin filament containing cardiac troponin and the various Tm dimers. For each Tm-dimer the measurement was done in the absence and presence of  $Ca^{2+}$  and showed little difference between the 3 Tm dimer filaments. These complex curves contain a large amount of information in addition to the rates of S1 binding, including the fraction of filament in the blocked state in the presence and absence of calcium and the number of S1's required to bind to activate the filament (34). However, since the curves are identical in each case a more complex analysis is unwarranted.

Controls using the  $\alpha$ - $\beta$ -Tm that had not been through the oxidation step showed that as reported previously the affinity for actin and the calcium regulation of myosin binding and not sensitive to the presence of the crosslink.

### Discussion

We have established here a reliable method for assembling and purifying an  $\alpha$ - $\beta$ -Tm heterodimer. This is important since human muscle tissue (cardiac and skeletal) contains both  $\alpha_2$ - and  $\alpha$ - $\beta$ -Tm and during disease or muscle remodelling following injury the proportion of  $\alpha_2$ - vs  $\alpha$ - $\beta$ -Tm can change. The functional consequence of the isoform shifts have not been defined- in part because of the unavailability of defined  $\alpha$ - $\beta$ -Tm samples for *in vitro* studies. This is no longer a limitation. The same method used here can also be used to assemble heterodimers carrying point mutation in one of the two chains either in  $\alpha$ - $\alpha$  or  $\alpha$ - $\beta$ -Tm. To date Tm mutations in  $\alpha$ - or  $\beta$ -Tm have only been characterized *in vitro* using the homodimer constructs where both chains carry the mutation. Yet the Tm mutations are normally present in a heterozygote background and a mixed population of dimers carrying zero ( $\alpha\alpha$  or  $\alpha\beta$ ), one ( $\alpha^*\beta$ ,  $\alpha^*\alpha$  or  $\alpha\beta^*$ ) or two copies ( $\alpha^*\alpha^*$ ) of the mutation is expected. The presence of a single point mutation in one vs two chains in the parallel Tm dimers could give quite distinct properties to the dimer. We have successfully used the method presented here to assemble an  $\alpha\alpha^*$  dimer where one chain carries a single point mutation associated with human cardiac cardiomyopathy (manuscript in preparation).

In the approach developed here a single chain carries an affinity tag on the N-terminus rather than each chain carrying different tags. We did investigate the two tag method (Strep-tag and His-tag on different Tm chains) for isolation of the heterodimer but we found that assembly of the heterodimer was greatly impaired when using two different tags. In addition the use of a single tag makes it easier to distinguish dimers with one two or zero tags from the size difference on SDS-gels.

This two tag method has been used for other protein heterodimers (e.g. myosin; (35)) but the single tag method works here for either the Strep or His tag constructs although the

separation of the one and two tagged Tm is not perfect. We have used the Strep tag here as the His-tag on  $\beta$ -Tm results in some degradation of the tagged protein during oxidation and during proteolysis of the tag. The preferential assembly of  $\alpha_2$ - and  $\alpha$ - $\beta$ -Tm using excess  $\alpha$ -Tm keeps the separation manageable and gives a reasonable yield of heterodimer. The tag was placed on the N-terminus since it is known that expression of fusion protein with large protein domains here do not disrupt Tm function whereas the C-terminus can be far more sensitive (36). The use of the Factor Xa protease allows removal of the Tag leaving no additional N-terminal amino acids apart from the Ala-Ser dipeptide to mimic the N-terminal acetylation.

The SDS-PAGE system originally used by Lehrer & colleagues (18), allows a simple assay for heterodimer formation and we have defined both the preference for homodimer over heterodimer formation and the effect of the tags on dimer formation. The data show a small preference for homodimer formation over  $\alpha$ - $\beta$  heterodimer and this is not greatly influenced by either of the single tags used. Using a combination of 50 %  $\alpha$ -Tm with 50 % tagged- $\alpha$ -Tm produced a mixture of dimers close to that predicted for random association (1 : 2 : 1 of  $\alpha_2$  :  $\alpha$ -tagged- $\alpha$  : tagged- $\alpha_2$ ; Janco, personal communication). In contrast a 50 : 50 mixture of  $\alpha$ - & tagged- $\beta$  monomers resulted in an approximately 2 : 1 : 2 mixture of  $\alpha_2$  :  $\alpha$ - $\beta$  :  $\beta_2$  dimers, independent of the presence of the tag - suggesting a mild preference for the homodimer assembly. This result for mammalian skeletal muscle Tm is in contrast to the frog skeletal muscle Tm which preferentially assembles into the heterodimer but only over a long period of incubation at 34 °C (half time 50 min.; (37)). Longer incubations did not improve the yield of heterodimer for the mammalian protein and this may reflect the smaller differences between the thermal stability of the three mammalian dimers (see discussion below). The avian smooth muscle Tm has a very strong preference for the  $\alpha$ - $\beta$  heterodimer assembly (38) and homodimers are rarely observed. Yet smooth Tm is expressed from the same two genes as the skeletal Tms but with alternate splicing of 2 of the 9 exons (3) (39). Thus the information to switch preference is contained in the alternate exons 2a and 9d used in smooth muscle Tm.

Tm binding to actin shows only small differences between the three Tm constructs. The two homodimers bind with quite tight apparent affinities 0.21 ( $\alpha_2$ -Tm) and 0.13 ( $\beta_2$ -Tm)  $\mu$ M similar to values reported in the past at this ionic strength (16). These values appear to be distinct but are close to the limit of the sensitivity of the method. In contrast the  $\alpha$ - $\beta$ -Tm has a significantly ( $p < 0.05$ ) weaker apparent affinity of 0.36  $\mu$ M. Although distinct this weaker affinity is unlikely to have physiological significance in a muscle fibre where the actin and Tm concentrations are much higher than this. Previous work from the group (40) also indicated that the presence of the Tm cross-link had little effect on actin affinity – at least at 20 °C.

The functional test of Tm together with Tn regulating the binding of myosin to actin shows no detectable differences between the three dimers. This is consistent with the work on intact mouse hearts which showed no deleterious effect of expressing up to 50 %  $\beta$  isoform which can be assumed to be predominantly  $\alpha$ - $\beta$  dimers (12). Expression of more the 50 %  $\beta$ -Tm will result in formation of  $\beta_2$ -Tm dimers and this is deleterious (13).

Thermal stability studies do show some interesting difference between the dimers but again the physiological significance is difficult to define. Our thermal transitions occur at a little higher temperature than those reported by DSC (23). The DSC used a lower ionic strength buffer (100 mM KCl) which can affect the stability of the protein (41). We use the higher ionic strength buffer (500 mM NaCl) to eliminate the end to end polymerization of the Tm samples and our data is similar to that of Hayley et al. (42) who used rabbit cardiac  $\alpha_2$ -Tm in 1 M KCl. Apart from the precise melting temperature the overall melting profile of our

$\alpha_2$ -Tm data is similar to that previously reported using DSC and CD for  $\alpha_2$ -Tm (23) (41) and related to the earlier work on frog and smooth muscle tropomyosin (18) (37) (38).

The heterodimers when cross-linked do show a distinct increased stability over that expected for the arithmetic sum of the two homodimers and this is particularly marked in the physiological range of temperature 35 - 45 °C. These differences are harder to define in the absence of the cross-link but are less marked— but the differences between  $\alpha_2$  and  $\beta_2$  are also smaller in the absence of the cross-link. The non cross-linked Tm is the normal state of Tm expected in the cell and this has recently been confirmed experimentally (43) (44). Cross-linking may occur under pathological conditions in which the level of reactive oxygen in tissues are elevated (45) (46). But it remains to be defined if the cross linking of Tm has any influence on muscle function. It is of interest to note in this respect that  $\alpha_2$ -Tm does show a small loss of stability in the temperature range of 35-40 °C on oxidation (see fig 5B). In contrast the oxidized  $\alpha\cdot\beta$ -Tm is a little more stable than the oxidized  $\alpha_2$ -Tm and in fact has similar stability at this temperature to the reduced  $\alpha\alpha$ -Tm. If Tm is susceptible to cross-linking under oxidative stress then expression of  $\alpha\cdot\beta$ -Tm could offer some protection. However, note that the non-cross-linked, reduced Tm is much less stable than reduced  $\alpha_2$ -Tm so that cross-linking would have to be quite extensive for the presence of  $\alpha\cdot\beta$ -Tm to be of advantage.

The work here does show a small but significant differences in the behavior of the  $\alpha\cdot\beta$ -Tm compared to the  $\alpha_2$ -Tm dimer. However, none of these appears sufficient on its own to explain why the cell varies the proportion of the two dimers under different conditions or why there is variation between the amount  $\alpha\cdot\beta$ -Tm present in different mammals.

Sequence comparison of human  $\alpha$ - &  $\beta$ -Tm shows little that might explain the different properties of  $\alpha$  &  $\beta$  Tm. There are 39 changes in sequence out of a total of 284 amino acids. Most changes are conservative, are in surface residues (i.e. not the core of the heptad repeats) and more of the changes (25 residues) are in the C-terminal half of the proteins. The region from 71 - 142 is the most conserved area with only 3 changes.

## Supplementary Material

Refer to Web version on PubMed Central for supplementary material.

## Acknowledgments

We would like to thank Samantha Lynn and Kevin Howland (both University of Kent, Canterbury, UK) for their technical assistance and Prof. Kornelia Jaquet (Ruhr-Universitaet Bochum, Bochum, Germany) for providing the human cardiac Troponin. This work was supported by the Wellcome Trust (Grant 085309) and the British Heart Foundation studentship to AK.

**Funding Source Statement:** This work was supported by the Wellcome Trust (Grant 085309) and the British Heart Foundation studentship to AK.

## Abbreviations

<b>Tn</b>	Troponin
<b>S1</b>	myosin subfragment 1
<b><math>\alpha_2</math>-Tm</b>	$\alpha$ Tropomyosin homodimers
<b><math>\beta_2</math>-Tm</b>	$\beta$ Tropomyosin homodimers
<b><math>\alpha\cdot\beta</math>-Tm</b>	$\alpha\cdot\beta$ Tropomyosin heterodimer

<b>His<math>\beta</math>-Tm</b>	Histidine-tagged $\beta$ -Tropomyosin
<b>Strep<math>\beta</math>-Tm</b>	Strep-tagged $\beta$ -Tropomyosin
<b>CV</b>	column volume

## References

- Gunning P, O'Neill G, Hardeman E. Tropomyosin-based regulation of the actin cytoskeleton in time and space. *Physiol Rev.* 2008; 88:1–35. [PubMed: 18195081]
- Bailey K. Tropomyosin; a new asymmetric protein component of the muscle fibril. *Biochem J.* 1948; 43:271–279. [PubMed: 16748400]
- Perry SV. Vertebrate tropomyosin: distribution, properties and function. *J Muscle Res Cell Motil.* 2001; 22:5–49. [PubMed: 11563548]
- Gordon AM, Homsher E, Regnier M. Regulation of contraction in striated muscle. *Physiol Rev.* 2000; 80:853–924. [PubMed: 10747208]
- Lewis WG, Smillie LB. The amino acid sequence of rabbit cardiac tropomyosin. *J Biol Chem.* 1980; 255:6854–6859. [PubMed: 6993480]
- Cummins P, Perry SV. The subunits and biological activity of polymorphic forms of tropomyosin. *Biochem J.* 1973; 133:765–777. [PubMed: 4270662]
- Cummins P, Perry SV. Chemical and immunochemical characteristics of tropomyosins from striated and smooth muscle. *Biochem J.* 1974; 141:43–49. [PubMed: 4218095]
- Bronson DD, Schachat FH. Heterogeneity of contractile proteins. Differences in tropomyosin in fast, mixed, and slow skeletal muscles of the rabbit. *J Biol Chem.* 1982; 257:3937–3944. [PubMed: 7061518]
- Leger J, Bouveret P, Schwartz K, Swynghedauw B. A comparative study of skeletal and cardiac tropomyosins: subunits, thiol group content and biological activities. *Pflugers Arch.* 1976; 362:271–277. [PubMed: 131298]
- Pieples K, Wieczorek DF. Tropomyosin 3 increases striated muscle isoform diversity. *Biochemistry.* 2000; 39:8291–8297. [PubMed: 10889038]
- Izumo S, Nadal-Ginard B, Mahadavi V. Protooncogene induction and reprogramming of cardiac gene expression produced by pressure overload. *Proc. Natl. Acad. Sci. USA.* 1988; 85:339–343. [PubMed: 2963328]
- Muthuchamy M, Grupp IL, Grupp G, O'Toole BA, Kier AB, Boivin GP, Neumann J, Wieczorek DF. Molecular and physiological effects of overexpressing striated muscle beta-tropomyosin in the adult murine heart. *J Biol Chem.* 1995; 270:30593–30603. [PubMed: 8530495]
- Muthuchamy M, Boivin GP, Grupp IL, Wieczorek DF. Beta-tropomyosin overexpression induces severe cardiac abnormalities. *J Mol Cell Cardiol.* 1998; 30:1545–1557. [PubMed: 9737941]
- O'Brien R, Sturtevant JM, Wrable J, Holtzer ME, Holtzer A. A scanning calorimetric study of unfolding equilibria in homodimeric chicken gizzard tropomyosins. *Biophysical Journal.* 1996; 70:2403–2407. [PubMed: 9172766]
- Nevzorov I, Redwood C, Levitsky D. Stability of two beta-tropomyosin isoforms: effects of mutation Arg91Gly. *J Muscle Res. Cell Motil.* 2008; 29:173–176. [PubMed: 19214762]
- Boussouf SE, Maytum R, Jaquet K, Geeves MA. Role of tropomyosin isoforms in the calcium sensitivity of striated muscle thin filaments. *J Muscle Res Cell Motil.* 2007; 28:49–58. [PubMed: 17436057]
- Eisenberg E, Kielley WW. Troponin-tropomyosin complex. Column chromatographic separation and activity of the three, active troponin components with and without tropomyosin present. *J Biol Chem.* 1974; 249:4742–4748. [PubMed: 4276966]
- Lehrer SS, Qian Y. Unfolding/refolding studies of smooth muscle tropomyosin. Evidence for a chain exchange mechanism in the preferential assembly of the native heterodimer. *J Biol Chem.* 1990; 265:1134–1138. [PubMed: 2295604]

19. Jansco A, Graceffa P. Smooth muscle tropomyosin coiled-coil dimers. Subunit composition, assembly, and end-to-end interaction. *J Biol Chem.* 1991; 266:5891–5897. [PubMed: 2005125]
20. Schmidt TG, Skerra A. The Strep-tag system for one-step purification and high-affinity detection or capturing of proteins. *Nat Protoc.* 2007; 2:1528–1535. [PubMed: 17571060]
21. Assouline Z, Graham R, Miller RCJ, Warren AJ, Kilburn DG. Processing of fusion proteins with immobilized factor Xa. *Biochemol Prog.* 1995; 11:45–49.
22. Monteiro PB, Lataro RC, Ferro JA, Reinach Fde C. Functional alpha-tropomyosin produced in *Escherichia coli*. A dipeptide extension can substitute the amino-terminal acetyl group. *J Biol Chem.* 1994; 269:10461–10466. [PubMed: 8144630]
23. Kremneva E, Boussouf S, Nikolaeva O, Maytum R, Geeves MA, Levitsky DI. Effects of two familial hypertrophic cardiomyopathy mutations in alpha-tropomyosin, Asp175Asn and Glu180Gly, on the thermal unfolding of actin-bound tropomyosin. *Biophys J.* 2004; 87:3922–3933. [PubMed: 15454401]
24. Sambrook, J.; Russe, DW. *Molecular Cloning: A Laboratory Manual.* 3rd ed. Cold Spring Harbor Press; Cold Spring Harbor, NY: 2001.
25. Clos J, Brandau S. pJC20 and pJC40-Two High-Copy-Number Vectors for T7 RNA-Polymerase-Dependent Expression of Recombinant Genes in *Escherichia coli*. *Protein Expression and Purification.* 1994; 5:133–137. [PubMed: 8054844]
26. Coulton AT, Koka K, Lehrer SS, Geeves MA. Role of the head-to-tail overlap region in smooth and skeletal muscle beta-tropomyosin. *Biochemistry.* 2008; 47:388–397. [PubMed: 18069797]
27. Coulton A, Lehrer SS, Geeves MA. Functional homodimers and heterodimers of recombinant smooth muscle tropomyosin. *Biochemistry.* 2006; 45:12853–12858. [PubMed: 17042503]
28. Laemmli UK. Cleavage of structural proteins during the assembly of the head of bacteriophage T4. *Nature.* 1970; 227:680–685. [PubMed: 5432063]
29. Spudich JA, Watt S. The regulation of rabbit skeletal muscle contraction. I. Biochemical studies of the interaction of the tropomyosin-troponin complex with actin and the proteolytic fragments of myosin. *J. Biol. Chem.* 1971; 246:4866–4871. [PubMed: 4254541]
30. Margossian SS, Lowey S. Preparation of myosin and its subfragments from rabbit skeletal muscle. *Methods Enzymol.* 1982; 85(Pt B):55–71. [PubMed: 6214692]
31. Criddle AH, Geeves MA, Jeffries T. The use of actin labelled with N-(1-pyrenyl)iodoacetamide to study the interaction of actin with myosin subfragments and troponin/tropomyosin. *Biochem J.* 1985; 232:343–349. [PubMed: 3911945]
32. Wegner A. Equilibrium of the actin-tropomyosin interaction. *J. Mol. Biol.* 1979; 131:839–853. [PubMed: 513132]
33. Ishii Y, Hitchcock-DeGregori SE, Mabuchi K, Lehrer SS. Unfolding domains of recombinant fusion alpha alpha-tropomyosin. *Protein Sci.* 1992; 1
34. Geeves M, Griffiths H, Mijailovich S, Smith D. Cooperative [Ca<sup>2+</sup>]-dependent regulation of the rate of myosin binding to actin: solution data and the tropomyosin chain model. *Biophysical Journal.* 2011; 100:2679–2687. [PubMed: 21641313]
35. Kad NM, Rovner AS, Fagnant PM, Joel PB, Kennedy GG, Patlak JB, Warshaw DM, Trybus KM. A mutant heterodimeric myosin with one inactive head generates maximal displacement. *The Journal of Cell Biology.* 2003; 162:481–488. [PubMed: 12900396]
36. Heald RW, Hitchcock-DeGregori SE. The Structure of the Amino Terminus of Tropomyosin Is Critical for Binding to Actin in the Absence and Presence of Troponin. *The Journal of Biological Chemistry.* 1988; 263:5254–5259. [PubMed: 2965699]
37. Lehrer SS, Qian Y, Hvidt S. Assembly of the Native Heterodimer of *Rana esculenta* Tropomyosin by Chain Exchange. *Science.* 1989; 246:926–928. [PubMed: 2814515]
38. Lehrer SS, Stafford WF 3rd. Preferential assembly of the tropomyosin heterodimer: equilibrium studies. *Biochemistry.* 1991; 30:5682–5688. [PubMed: 2043610]
39. Lees-Miller JP, Helfman DM. The molecular basis for tropomyosin isoform diversity. *Bioassay.* 1991; 13:429–437.
40. Boussouf, SE. Regulation of cardiac muscle contraction. University of Kent; UK: 2004. PhD thesis

41. Ishii Y. The local and global unfolding of coiled-coil tropomyosin. *Eur J Biochem.* 1994; 221:705–712. [PubMed: 8174550]
42. Hayley M, Chevaldina T, Heeley DH. Cold Adaption of Tropomyosin. *Biochemistry.* 2011; 50:6559–6566. [PubMed: 21707054]
43. Lehrer SS, Ly S, Fuchs F. Tropomyosin is in a reduced state in rat cardiac muscle. *J Muscle Res Cell Motil.* 2011; 32:63–64. [PubMed: 21789684]
44. Lehrer SS, Ly S, Fuchs F. Tropomyosin is in a reduced state in rabbit psoas muscle. *J Muscle Res Cell Motil.* 2011; 32:19–21. [PubMed: 21590498]
45. Canton M, Menezza S, Sheeran FL, Polverino de Laureto P, Di Lisa F, Pepe S. Oxidation of Myofibrillar Proteins in Human Heart Failure. *Journal of American College of Cardiology.* 2011; 57:300–309.
46. Canton M, Skyschally A, Menabo R, Boengler K, Gres P, Schula R, Haude M, Erbel R, Di Lisa F, Heusch G. Oxidative modification of tropomyosin and myocardial dysfunction following coronary microembolization. *European Heart Joournal.* 2006; 26:875–881.

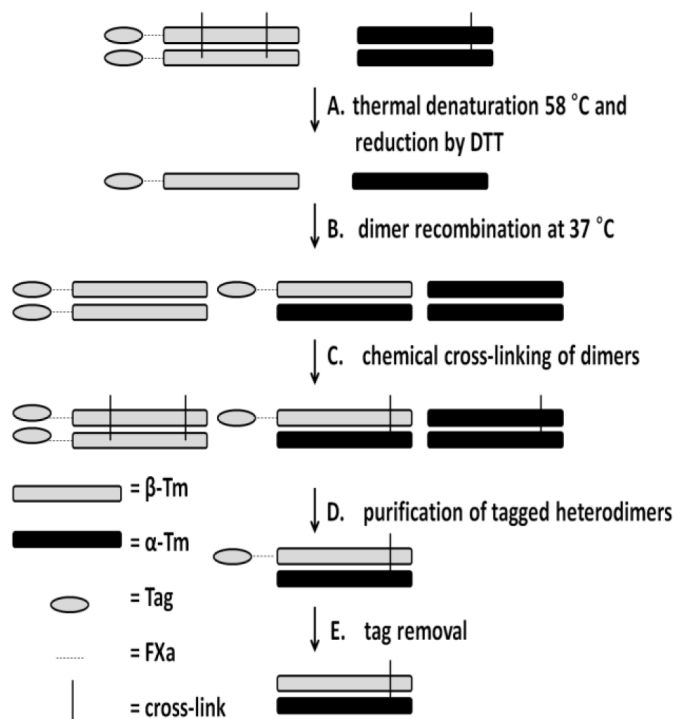


**Figure 1. Outline of the protocol for assembling and purifying  $\alpha$ - $\beta$ -Tm**

Starting with the bacterially expressed  $\alpha_2$ -Tm and tagged- $\beta_2$ -Tm the proteins were A) thermally denatured at 58 °C in the presence of DTT to generate Tm monomers. B) The Tm monomers were mixed in a ratio of 1 : 3 with  $\alpha$ -Tm in excess and incubated at 37 °C to allow dimer formation and then C) catalytically cross-linked at the Cys residues to trap the dimers. Note that  $\alpha$ -Tm has a single Cys (position 190 in the native-untagged Tm sequence) while  $\beta$ -Tm has two (at positions 36 and 190 in the native-untagged Tm sequence) resulting in a single crosslink for  $\alpha_2$ - and  $\alpha$ - $\beta$ - and a double crosslink in  $\beta_2$ -Tm. D) The Tm dimers were then separated using an affinity column for their respective tag and E) the isolated  $\alpha$ - $\beta$ -Tm was further subjected to an enzymatic proteolysis for the removal of the affinity tag.



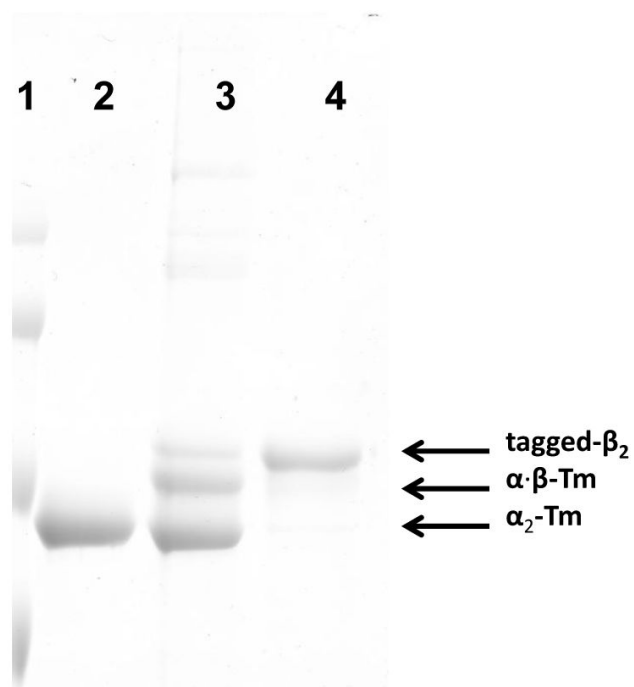


**Figure 2. SDS-gel of cross-linked dimers**

Lane 2 and 4 show the  $\alpha_2$ - and tagged- $\beta_2$ -Tm, respectively. Lane 3 shows the dimers formed after mixing, denaturing and recombining  $\alpha$ - and tagged- $\beta$ -monomers in a 3 : 1 ratio. The two homodimer bands (compare to lane 2 and 4) are shown plus the new band of the  $\alpha$ -tagged- $\beta$ -Tm, running between the two homodimer bands. Lane 1 contains a prestained protein ladders (PageRuler<sup>TM</sup> prestained protein ladder, Fermentas). Sample were separated on a non-reducing 7.5 % (w/v) SDS-gel.

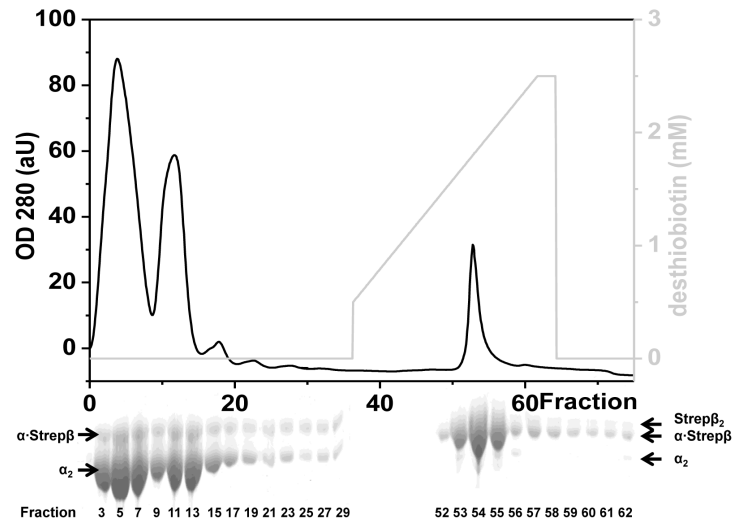


**Figure 3. SDS-gels of the affinity purification of  $\alpha$ -Strep $\beta$ -Tm**

After loading the mixture of  $\alpha_2$ -, Strep $\beta_2$ - and  $\alpha$ -Strep $\beta$ -Tm onto a Strep-Tactin-Sepharose column, the elutants were collected and run on a 7.5 % (w/v) non reducing SDS-gels. Any unbound dimers were washed off (Fraction 3-29). The  $\alpha$ -Strep $\beta$ -Tm elutes around 1.75 mM desthiobiotin as a heterodimer (Fraction 52-54) and with increasing of the desthiobiotin concentration Strep $\beta_2$ -Tm starts to co-elute (Fraction 55-62).

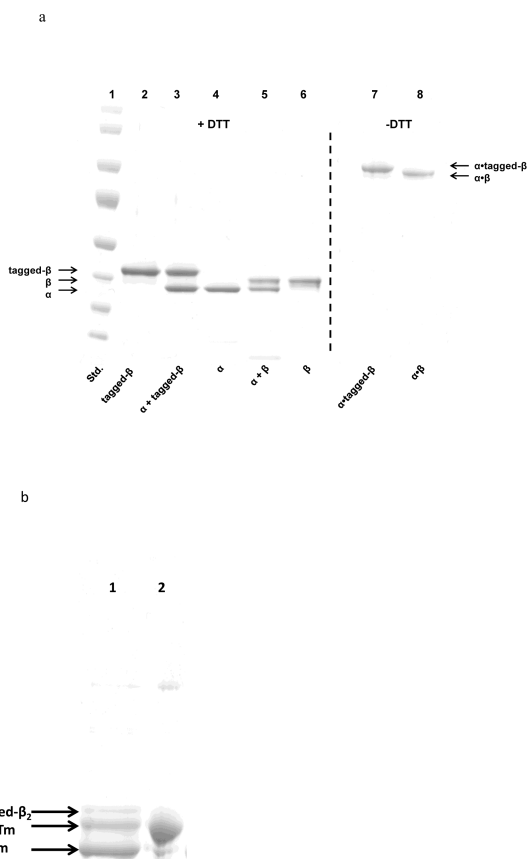


**Figure 4. SDS-gel of purified  $\alpha$ -tagged  $\beta$ -Tm and  $\alpha$ - $\beta$ -Tm heterodimers**

A: Purified tagged and untagged  $\alpha$ - $\beta$ -Tms run on a 12-4 % (w/v) SDS-gel under non reducing (lane 7 and 8) and reducing conditions (lane 3, 5).  $\alpha_2$ -Tm (lane 4), tagged- $\beta_2$ -Tm (lane 2) and  $\beta_2$ -Tm (lane 6) were loaded as controls under reducing conditions. Lane 1 contains a prestained protein ladders (PageRuler™ prestained protein ladder, Fermentas). B: Lane 2 shows purified  $\alpha$ -tagged- $\beta$ -Tm. Lane 1 shows a mixture of  $\alpha_2$ -Tm,  $\alpha$ - $\beta$ -Tm and tagged- $\beta_2$ -Tm as a control. Samples were separated on a 7.5 (w/v) SDS-gel under non reducing conditions.

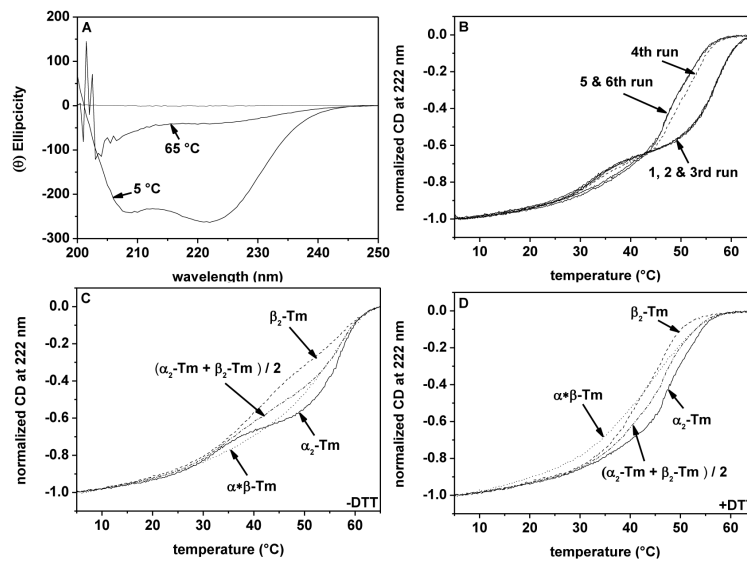


**Figure 5. Thermal unfolding of Tm dimers**

A) CD spectra of 10  $\mu\text{M}$   $\alpha$ -Tm. B) 6 scans at 222 nm of  $\alpha_2$ -Tm unfolding; three in the absence of DTT (run 1 - 3) followed by 3 in the presence of 1 mM DTT (run 4 - 6). C & D) Unfolding curves of  $\alpha$ - $\beta$ -,  $\alpha_2$ - and  $\beta_2$ -Tm and the predicted unfolding curve for a 50 : 50 mixture of  $\alpha_2$ - and  $\beta_2$ -Tm are shown in the absence (C) and presence (D) of 1 mM DTT. Each unfolding curve in C & D is the 3<sup>rd</sup> of three repeats on the same sample. Buffer: 0.5 M NaCl, 5 mM  $\text{MgCl}_2$ , 20 mM potassium phosphate buffer, pH 7.0.

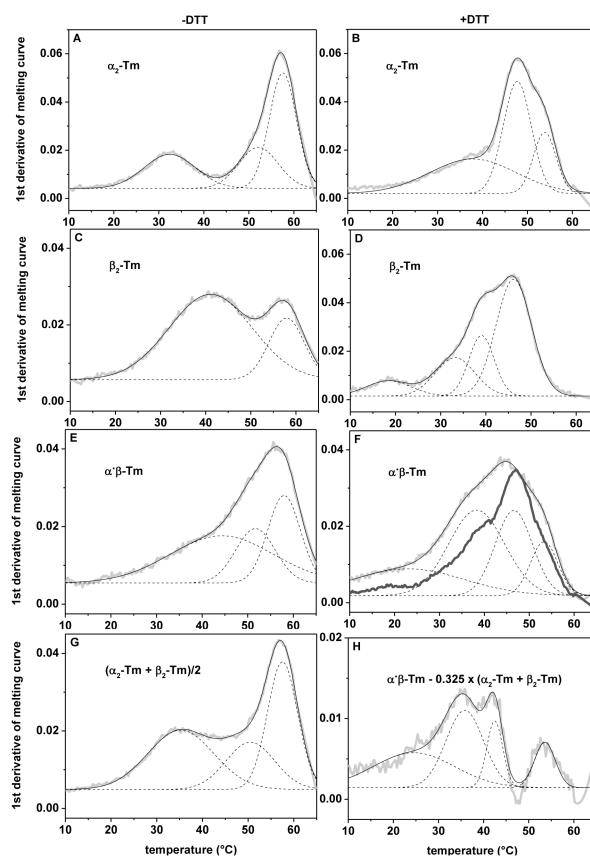


### Figure 6. Thermal unfolding domains of Tm dimers

The 1st derivative calculated for each melting curve presented in Figure 5 with best fit to multiple Gaussian peaks. A summary of the fitted parameters is given in Table 1.

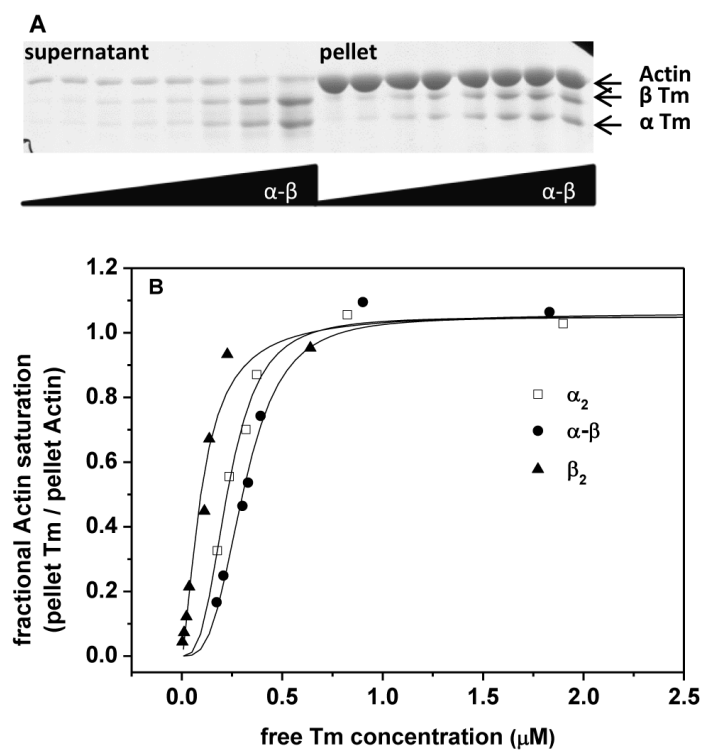


**Figure 7. Estimation of the affinity of Tm for actin**

Actin ( $7 \mu\text{M}$  for  $\alpha\text{-}\beta$  and  $10 \mu\text{M}$  for  $\alpha_2$ - or  $\beta_2$ -Tm) was incubated with increasing concentrations of Tm dimers at  $20^\circ\text{C}$  for 1h in 20 mM MOPS, pH 7.0, 100 mM KCl, 5 mM  $\text{MgCl}_2$ . A) The actin and the fraction of Tm bound to it was pelleted at  $370000 \times g$  and equivalent volumes of the pellet and the supernatant were loaded onto a 7.5 % (w/v) reducing SDS-gel. B) For each experiment the fraction of Tm bound to actin was plotted against the free Tm concentration that was found in the supernatant. The actin binding affinity ( $K_d$ ) and the Hill coefficient ( $n$ ) values were calculated by fitting to the Hill equation and are listed in Table 2. Raw data are depicted with symbols and the Hill fits with lines.

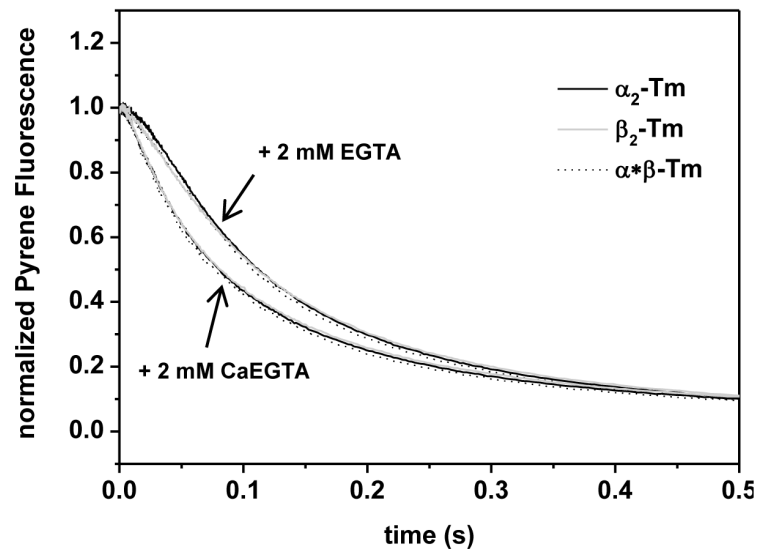


**Figure 8. Transients of S1 Binding to regulated (actin + various Tm + cardiac Tn) thin filaments** 0.25  $\mu\text{M}$  actin was preincubated with various Tm isoforms and cTn and pushed against 5  $\mu\text{M}$  S1 (concentrations after mixing). The binding of S1 to actin was measured in the absence of  $\text{Ca}^{2+}$  (2 mM EGTA) and in the presence of 2 mM Ca.EGTA. The experimental buffer used for this experiment was 100 mM KCl, 5 mM  $\text{MgCl}_2$ , 20 mM MOPS, pH 7.0.

**Table 1**  
**Thermal unfolding of Tm dimers**

The melting curves of the various Tm-dimers were smoothed (Savitzky-Golay method; 50 points of window), the 1<sup>st</sup> derivatives were calculated and multiple Gaussian peaks fitted. The width of the half peak, the peak midpoint and their respective standard errors are given in °C. The errors of the peak areas are expressed in % of the individual peak area.

	Oxidized TM –DTT			Reduced samples + DTT		
	Fractional Peak area (%)	Width of half peak (°C)	Peak midpoint (°C)	Fractional Peak area (%)	Width of half peak (°C)	Peak midpoint (°C)
$\alpha_2$ -Tm	27.6 ± 5 25.3 ± 32.2 48 ± 16	11.4 ± 0.3 8.7 ± 1.3 6 ± 0.2	32.4 ± 0.1 52.1 ± 1.4 57.5 ± 0.1	39.5 ± 11.8 41.9 ± 5.6 18.6 ± 12.5	19.2 ± 1.6 6.2 ± 0.2 5 ± 0.2	37.9 ± 0.8 47.7 ± 0.2 53.8 ± 0.2
$\beta_2$ -Tm	76.9 ± 1.9 23.5 ± 1.3	18.5 ± 0.2 7.8 ± 0.1	41.1 ± 0.1 57.9 ± 0.04	8.9 ± 12.5 18.9 ± 36 20 ± 22.2 52.2 ± 2.1	9.9 ± 0.6 8.8 ± 1.1 5.6 ± 0.3 7.8 ± 0.1	18.5 ± 0.3 33.2 ± 0.8 39 ± 0.1 46.2 ± 0.1
$\alpha$ - $\beta$ -Tm	50 ± 8.6 21.4 ± 20 28.6 ± 20	22.7 ± 1 8.6 ± 0.7 7.1 ± 0.3	44.3 ± 0.9 51.7 ± 0.9 58 ± 0.3	24.4 ± 54.4 37.8 ± 50 25.6 ± 52.2 12.2 ± 27.3	24.8 ± 9 12.5 ± 2.4 8.3 ± 1.4 6.1 ± 0.4	23.1 ± 5.9 38.3 ± 1.6 46.6 ± 0.3 53.3 ± 0.4
Predicted -DTT ( $\alpha_2$ -Tm + $\beta_2$ -Tm) / 2 +DTT $\alpha$ - $\beta$ -Tm – 0.325 * ( $\alpha_2$ -Tm + $\beta_2$ -Tm)	39.4 ± 3.6 22.5 ± 25 38.1 ± 11	14.4 ± 0.4 10.6 ± 1.5 6.6 ± 0.2	35.3 ± 0.3 50.5 ± 0.9 57.5 ± 0.1	36.7 ± 31.4 37.6 ± 26.9 13.7 ± 16 12 ± 9.1	18 ± 4 8.3 ± 1.1 3.5 ± 0.3 4.6 ± 0.4	24.5 ± 2.7 35.8 ± 0.3 42.5 ± 0.1 53.6 ± 0.2
Strep $\beta_2$ -Tm	69.6 ± 4.2 17.4 ± 8.3 13 ± 11.1	20.7 ± 0.6 6.3 ± 0.2 6.9 ± 0.2	39 ± 0.4 47.5 ± 0.05 58 ± 0.1	10.9 ± 10 57.6 ± 3.8 5.4 ± 20 26.1 ± 4.1	11.6 ± 0.5 15.3 ± 0.4 4.6 ± 0.3 6.3 ± 0.1	19.8 ± 0.3 40.6 ± 0.3 40.7 ± 0.1 48.5 ± 0.04
$\alpha$ -Strep $\beta$ -Tm	26.9 ± 2.2 35.8 ± 4.2 37.3 ± 4	10.6 ± 0.2 8.8 ± 0.3 7.4 ± 0.1	33.7 ± 0.1 49.3 ± 0.2 58.3 ± 0.1	28.8 ± 16.7 5.6 ± 42.9 16.8 ± 14.3 48.8 ± 4.9	26.5 ± 3.4 9.1 ± 1.5 6.5 ± 0.2 13.7 ± 0.5	22.6 ± 1.5 34.9 ± 0.8 47.8 ± 0.1 47.9 ± 0.3
Predicted -DTT ( $\alpha_2$ -Tm + Strep $\beta_2$ -Tm) / 2 +DTT $\alpha$ -Strep $\beta$ -Tm – 0.325 * ( $\alpha_2$ -Tm + Strep $\beta_2$ -Tm)	38 ± 3.7 25.4 ± 5.6 36.6 ± 3.8	14.5 ± 0.3 8.4 ± 0.3 6.3 ± 0.1	34.2 ± 0.2 48.8 ± 0.1 57.5 ± 0.1	100 ± 1	8.5 ± 0.1	47.6 ± 0.1



**Table 2**  
**Estimation of the affinity of Tm for actin**

For each Tm dimer the cosedimentation experiment of Figure 7 was repeated 3 times and the mean values of the actin binding affinity ( $K_{50\%}$ ) and the apparent Hill coefficient ( $n$ ) together with their SD errors are summarized.

Tm dimers	$K_{50\%}$ ( $\mu\text{M}$ )	Apparent Hill coefficient $n$
$\alpha_2$ ( $n = 3$ )	$0.21 \pm 0.02$	$3.5 \pm 1.1$
$\alpha\text{-}\beta$ ( $n = 3$ )	$0.36^* \pm 0.07$	$2.4 \pm 0.7$
$\beta_2$ ( $n=3$ )	$0.13 \pm 0.06$	$1.6 \pm 0.1$

\* t-test  $p < 0.05$  for  $\alpha\text{-}\beta$   $K_{50\%}$  compared to either  $\alpha_2$ - or  $\beta_2$ -Tm. All other comparisons are  $p > 0.05$ .